ORIGINAL CONTRIBUTION

Synthesis of silica-coated ZnO nanocomposite: the resonance structure of polyvinyl pyrrolidone (PVP) as a coupling agent

Jinfeng Wang · Takuya Tsuzuki · Bin Tang · Pavel Cizek · Lu Sun · Xungai Wang

Abstract The preparation of silica-coated ZnO nanocomposite using polyvinyl pyrrolidone (PVP) as a coupling agent was investigated. Transmission electron microscopy analysis revealed that silica has been deposited on the surface of PVP-capped ZnO nanoparticles as a continuous thin layer. Two-dimensional correlation analysis based on the time-dependent UV–vis spectra was introduced to study the interaction governing the deposition of silica on to PVP-capped ZnO. Strong hydrogen bonds formed between the amphiphilic PVP molecules and silica in the silica-coated PVP-capped ZnO composites. The reduced photocatalytic activity of silica-coated ZnO nanoparticles will enhance their performance as durable, safe, and non-reactive UV blockers in plastics, paints, and coating for outdoor textile and timber products.

Keywords ZnO nanoparticles · PVP · Coupling agent · Photocatalytic activity

Introduction

Silica coating of nanoparticles has been widely studied on some materials such as Fe_2O_3 and TiO_2. In industry, silica-coated TiO_2 has a rather long history in various applications [1]. However, the application of silica coating on ZnO is significantly more difficult than TiO_2 or other chemically stable materials [2, 3]. In order to apply silica coating on each particle, it is necessary to achieve a high degree of particle dispersion. However, since ZnO has a high solubility in acid or base solutions, it is difficult to obtain high dispersion stability of ZnO particles in ethanol or water suspensions by using electrostatic repulsion force through controlling pH [1, 4, 5]. Graf et al. reported that polyvinyl pyrrolidone (PVP) could be used as a dispersant to improve the dispersion stability of colloid particles to perform silica coating in ethanol media [6]. PVP can be adsorbed onto a broad range of materials such as metals (e.g., gold, silver, and iron), metal oxides (kaolinite, TiO_2, iron oxide, and alumina) [7], polystyrene [8], silica [9], and graphite [10]. It stabilizes colloidal particles in water and many nonaqueous solvents. Hence, the use of PVP as a coupling agent is expected to be a versatile, simple, and fast technique to coat colloidal particles with silica.

In this article, the use of PVP as a coupling agent between ZnO and silica is investigated to fabricate silica-coated ZnO nanoparticles. In the past, some amphiphilic noninonic polymers have been used as a coupling agent for applying silica coating on colloidal particles. However, to the best of our knowledge, this is the first time that this approach has been successfully taken to overcome the chemical instability and poor dispersion characteristics of ZnO nanoparticles during silica coating. We discuss the coupling mechanism by addressing how a PVP segment transfers between its two resonance structures during the silica-shell growth process [6, 11].

The application of silica coatings on ZnO nanoparticles is of great importance for the effective control of the photocatalytic activity of ZnO, in particular, for UV-protection applications. Due to its ability to absorb a wide spectrum of UV light as well as its physical and chemical stability under both high temperature and UV irradiation,

J. Wang · T. Tsuzuki · B. Tang · P. Cizek · L. Sun (✉) · X. Wang
Centre for Material and Fibre Innovation, Institute for Technology
Research and Innovation, Deakin University,
Geelong, Victoria 3217, Australia
e-mail: lu.sun@deakin.edu.au

there has been immense commercial and academic interest in applying ZnO as an effective UV absorber [12, 13] However, the practical application is still limited because of the inherent photocatalytic activity that may cause damage to skin and surrounding organic matrices [14, 15]. Silica coating on ZnO is expected to reduce the photocatalytic activity by confining photo-induced charge carriers inside the coating. Hence, in this article, we also explore the relationship between the silica-shell thickness and the photocatalytic activity of silica–ZnO nanocomposites.

Experimental section

Synthesis of PVP-capped ZnO nanoparticles

First, 0.27 g of $Zn(Ac)_2 \cdot 2H_2O$ was dissolved in ethanol and heated to 60 °C under constant stirring for 2 h. Then, 0.5 g of PVP was added to the solution. After the PVP was dissolved in ethanol, the solution was cooled down to room temperature. A NaOH solution was prepared separately by dissolving 0.098 g of $NaOH \cdot H_2O$ in 50 ml of ethanol at room temperature in an ultrasonic bath. The NaOH solution was added dropwise into the $Zn(Ac)_2$ solution under constant stirring to form PVP-capped ZnO nanoparticles. The solution mixture was then stirred continuously at room temperature for up to 2 h. The PVP-capped ZnO particles were flocculated from ethanol by the addition of hexane (30 ml of hexane/10 ml of reaction mixture) and subsequently separated by centrifugation at 6,000 rpm for 10 min. The particles were rinsed with ethanol once again and finally collected after centrifuging at 6,000 rpm for 10 min.

Synthesis of silica-coated ZnO nanocomposite (silica–ZnO nanocomposite)

The growth of silica layers on colloidal particles was performed based on the Stöber method [16]. The PVP-capped ZnO nanoparticles were re-dispersed in ethanol that contained 4.2 vol.% of aqueous ammonia solution (29.3 wt.% NH_3 in water), immediately followed by the addition of a tetraethylorthosilicate (TEOS) solution (10 vol.% in ethanol) under stirring at 600 rpm. The reaction mixtures were then aged while stirring for different time periods ranging from 7 to 48 h.

Characterization

X-ray diffraction (XRD) spectra of PVP-capped ZnO nanoparticles before and after silica coating were obtained using a Phillips PW-1729 diffractometer (35 kV, 28 mA) with Cu-Kα radiation at room temperature at a scanning rate of $2.4° min^{-1}$.

The morphologies and structures of the samples were studied by transmission electron microscopy (TEM) using a JEM-2100 microscope operated at an acceleration voltage of 200 kV. Samples were prepared by placing a drop of aqueous particle suspension onto a carbon coated copper grid followed by drying at room temperature. The optical absorption spectra of the samples were obtained using a Varian Cary 3E UV–vis spectrophotometer. Fourier transform infrared (FT-IR) spectra were measured with a Bruker Vertex 70 FT-IR spectrophotometer, using the KBr method.

Two-dimensional correlation analysis

The UV–vis absorption spectra of the samples aged in the range of 0–48 h in the silica coating process were analyzed using the two-dimensional (2D) correlation analysis method [17] without any further pretreatment. In the present study, the 2D correlation spectra were calculated by the 2D Shige software developed by Dr Shigeaki Morita (Yukihiro Ozaki group, Kwansei-Gakuin University, Japan, http://sci-tech.ksc.kwansei.ac.jp/~ozaki/2D-shige.htm).

Photocatalytic activity test

Rhodamine B (RhB) was used as a probe molecule to evaluate the photocatalytic activity of uncoated and silica-coated ZnO nanoparticles in response to UV and visible light irradiation. The characteristic optical absorption peak of RhB at 554 nm was chosen to monitor the photocatalytic degradation process. The experiment was carried out according to the following procedure: 8 mg of the dried powder was dispersed in 50 mL of RhB aqueous solution in a 100-mL beaker (for all photodegredation experiments, the amount of ZnO was maintained to be the same). The suspension was stirred in the dark for 1 h to ensure the establishment of adsorption and desorption equilibrium of RhB on the particle surface. Subsequently, the suspension was irradiated with simulated sunlight using an Atlas Suntest CPS1 instrument equipped with 150-W xenon lamp and a filter (coated quartz dish). At given intervals, 3 mL of the suspension was extracted and then centrifuged at 6,000 rpm for 10 min to separate the nanoparticles from the supernatant. UV–vis specular absorbance spectra of the supernatant were measured with a Varian Cary 3E spectrophotometer.

Results and discussion

Crystal structure and compositions of silica-coated ZnO nanocomposites (silica–ZnO nanocomposites)

Figure 1 shows XRD spectra of PVP-capped ZnO nanoparticles before and after silica coating. The diffraction
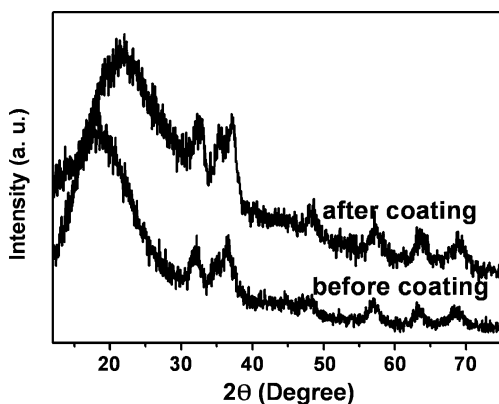
Fig. 1 X-ray diffraction patterns of PVP-capped ZnO nanoparticles before and after silica coating

patterns of both samples exhibit the peaks corresponding to the Wurtzite structure (JCPDS card 36-1451). These peaks are broad, suggesting that the crystallites have sizes in the nanometer range. The broad diffraction peaks of the sample after coating confirmed that the crystal structure of ZnO nanoparticles was not altered during the silica coating process.

Figure 2 shows the TEM micrographs of the PVP-capped ZnO nanoparticles before and after silica coating. The coated sample was aged for 24 h. As shown in Fig. 2a, all the PVP-capped ZnO particles were nearly spherical in morphology. The corresponding high-magnification TEM image revealed that the lattice fringes of the particles were in the same direction across the whole structure, indicating that the particles were single crystals. In the TEM image of the sample after coating (Fig. 2b), the silica layers are evident as the gray network structure and PVP-capped ZnO cores appear as the small dark dots. It can be seen that roughly spherical nanoparticles are homogeneously dispersed in the silica matrix. Instead of individually dispersed silica-shell/ZnO-core nanoparticles, a silica–ZnO nanocomposite with a network structure was obtained. Assuming that the weight ratio between PVP and ZnO remained the same before and after silica coating, thermogravimetric
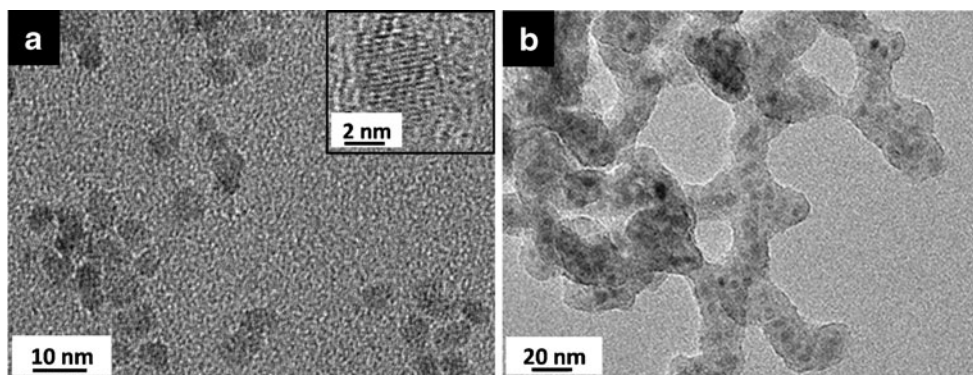
analysis suggested that the amount of ZnO in the composite was 8 wt.% (Fig. S1 in the supporting information).

The interaction between PVP, silica, and ZnO during silica coating process

Figure 3 shows time-dependent UV–vis absorption spectra of the coated samples with different coating times. After 7 h of coating time, the absorbance intensity at 350 nm decreased by ~15%. This decrease in the UV absorption indicates the loss of ZnO nanoparticles. It is speculated that a small amount of ZnO reacted with NH_4OH to transform into a zinc ammonium hydroxide complex, which does not absorb UV light [18]. When the coating time was prolonged from 7 to 48 h, the absorbance intensity at 350 nm remained constant. The absorbance intensity at 350 nm did not change even after several weeks. This indicates that, after aging for 7 h, silica coating was sufficiently developed on ZnO nanoparticles to prevent further reaction between ZnO and NH_4OH. Figure 3 also shows that the absorbance intensity in the region between 370 and 600 nm increased as the aging time was prolonged from 7 to 48 h. Since the bandgap wavelength of ZnO is ~370 nm, the absorbance above this wavelength is mostly due to the light scattering. Hence, the change in the absorbance intensity in the region between 370 and 600 nm is attributed to the increase of light-scattering intensity due to the increase of the silica-layer thickness and agglomeration of silica-coated nanoparticles [19].

Two-dimensional correlation analysis is useful for simplifying overlapped peaks and determining the change sequence of the peaks [17]. Hence, in order to gain further insight into the transition structure of PVP molecules, 2D correlation analysis was performed for the time-dependent UV–vis spectra during the silica coating process. The synchronous and asynchronous maps in the region of 200–600 nm are obtained, as shown in Fig. 4. The contours in the figures indicate the relative changes in the UV absorption spectrum at a fixed time interval. In the synchronous map (Fig. 4a), two auto-correlation peaks are evident at ~270 and ~375 nm
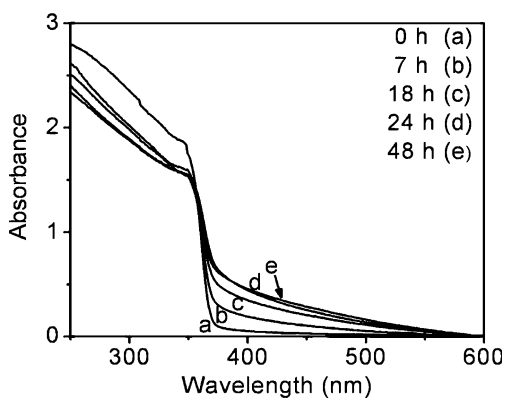

Fig. 2 Transmission electron microscopy images of PVP-capped ZnO nanoparticles **a** before coating (*inset* shows a high-magnification lattice fringe image of a nanoparticle) and **b** after coating

Fig. 3 Time-dependent UV–vis absorption spectra during the silica coating process of PVP-capped ZnO nanoparticles

(indicated with arrows a and b), which indicates that the absorption intensity at ~270 and ~375 nm in the UV spectra changed during the process of the reaction. The cross-peak located at $(x, y) = (270, 375)$ nm is negative, suggesting that the change in the absorption intensity at those two wavelengths are in the opposite directions, i.e., one is increased while the other is decreased. As shown in Fig. 3, the light-scattering intensity above 370 nm increased with increasing aging time for silica coating, which is represented in the 2D correlation spectra by the increase of the peak intensity at 375 nm. Since the spectral variations at those two wavelengths are in the opposite directions, it is implied that the UV absorption intensity at 270 nm decreased during the coating process. It is to be noted that the peak at 270 nm in the 2D correlation spectra is not noticeable in the individual UV–vis spectra in Fig. 3, because the peak in the 2D correlation spectra could highlight only the relative change that is even invisible in UV–vis spectra.

In order to elucidate the origin of the peak at 270 nm in the time-correlation spectrum in Fig. 4a, the UV–vis absorption properties of PVP molecules were investigated in an ethanol–NaOH solution and in an ethanol solution

without NaOH. As shown in Fig. 5, PVP in the ethanol–NaOH solution exhibits a broad absorption band at 270 nm as indicated with arrows in the figure, which is nearly the same wavelength as the synchronous correlation peak in Fig. 4a. On the other hand, PVP in the ethanol solution without NaOH did not show the absorption band at 270 nm. The main absorption peak of the PVP in the ethanol solution without NaOH was at 207 nm, 23 nm lower than that of PVP in the ethanol–NaOH solution. This red shift of the absorption peak is considered to be caused by the aggregation of the PVP molecules.

The origin of the peak at 270 nm in the synchronous correlation in Fig. 4a was further investigated through observation of the interaction between PVP-capped ZnO nanoparticles and silica layers by FT-IR spectroscopy. Figure 6 compares FT-IR spectra of silica alone, uncoated PVP-capped ZnO nanoparticles, and silica–ZnO nanocomposites. In the spectrum of uncoated PVP-capped ZnO nanoparticles (curve b in Fig. 6), the peaks labeled with 1–5, located at 3,450, 2,930, 1,675, 1,420, and 1,290 cm^{-1}, are assigned to the O–H stretching vibration, CH$_2$ unsymmetrical stretching vibration, C=O stretching vibration, CH$_2$ bending vibration, and C–N stretching vibration band, respectively [20, 21]. In the spectrum of silica–ZnO nanocomposite (curve c in Fig. 6), the C=O stretching band (peak 3) of PVP shifted from 1,675 to 1,653 cm^{-1}, indicative of the formation of intermolecular hydrogen bonds between OH groups on silica and C=O groups on PVP molecules [22].

These observations, together with previously published works on nanocomposites through PVP molecules as surfactant [6, 7, 20], suggest that for the development of silica shells, the PVP played a critical role. The mechanism of silica-layer formation can be described as follows. The PVP molecules may take resonance structures as shown in Fig. 7 [7].

In polar solvents such as NaOH/ethanol solution or aqueous ammonia solution in ethanol, the structure in which the electron spin density is localized on the nitrogen (b) is

Fig. 4 a–b Synchronous (*left*) and asynchronous (*right*) maps of 2D correlation spectra based on auto-correlation calculated from the time-resolved spectra in Fig. 3. The *shadowed areas* of cross-peak indicate negative correlation of two peaks, while the *unshadowed areas* represent positive correlations of two peaks
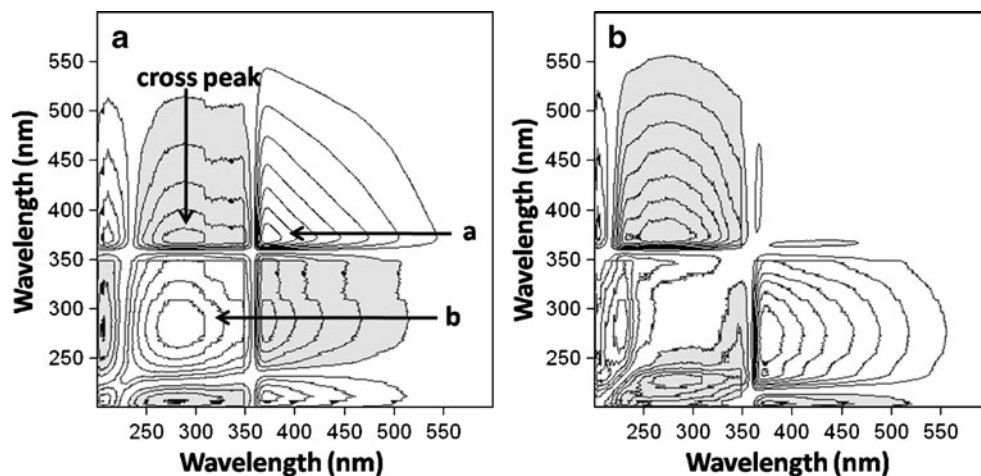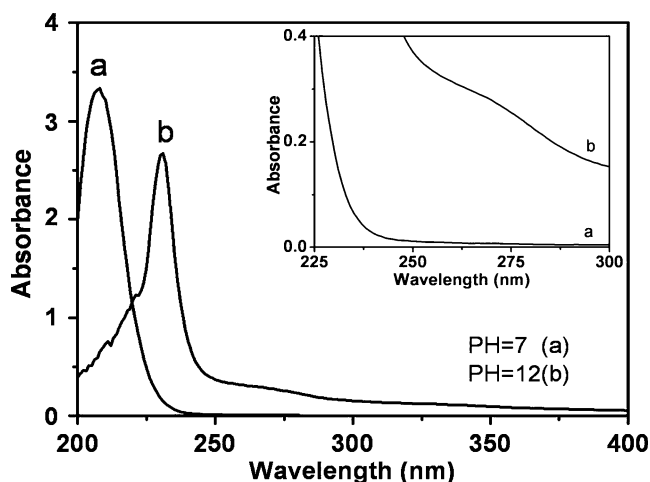
Fig. 5 UV–vis absorption spectra of PVP (a) ethanol solution and (b) pH=12 NaOH–ethanol solution

Fig. 7 a–b Resonance structures of a pyrene ring in PVP molecule

favored over the charge neutral structure (a), allowing the pyrene rings in PVP to have hydrophilic $=N^+$–C–O^- bond (Fig. 7b) [23]. According to the UV–vis measurements in Fig. 5, this structure (b) gives rise to the optical absorption at 270 nm. During the formation of ZnO nanoparticles in the presence of PVP, Zn^{2+} cations attach to the negatively charged C–O^- group in PVP and then Zn^{2+} transforms to ZnO through the reaction with OH ions [24]. While ZnO nanoparticles grow, PVP molecules remain attached to the Zn^{2+} sites on the particle surface by electrostatic interaction between the Zn^{2+} sites and the negatively charged C–O^- groups in PVP molecules.

During the formation of silica layers on PVP-capped ZnO nanoparticles, ammonia was gradually consumed for the hydrolysis of TEOS or evaporated, slowly reducing the polarity of the solution. Hence, the non-polar resonance structure (a) of pyrene rings in PVP becomes more favorable, which reduces the optical absorption intensity at 270 nm. At the same time, hydrogen bonds are formed between the silanol groups on hydrolyzed TEOS and C=O
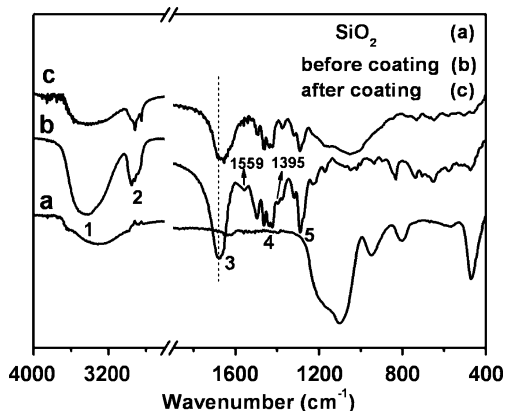

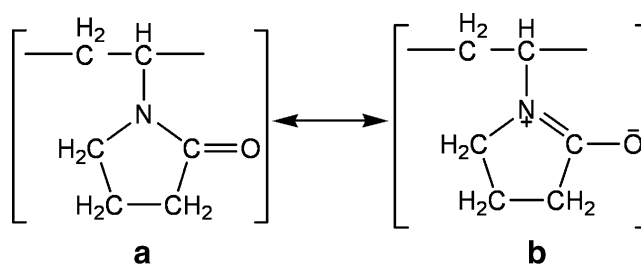Fig. 6 FT-IR spectra of (a) silica alone and PVP-capped ZnO, (b) before, and (c) after silica coating

groups in PVP molecules, as evident in the peak shift in FT-IR spectra, which may alter the electron energy states in the pyrene rings to further reduce the optical absorption intensity at 270 nm. This hydrogen bonding greatly assists the formation of silica layers on ZnO nanoparticles as the key mechanism of PVP's coupling function [7]. Hence, as the hydrolysis of TEOS and silica coating on ZnO progress, the number of the resonance structure (b) in PVP decreases, causing the decrease in light absorption intensity at 270 nm.

Photocatalytic activities of silica–ZnO nanocomposites with different silica-layer thickness

Four samples with different silica-layer thickness (Fig. S2 in the supporting information) were prepared with aging times of 7, 18, 24, and 48 h and herein denoted as SCZNs-7, SCZNs-18, SCZNs-24, and SCZNs-48, respectively. Figure 9a shows the relative change of the absorption peak intensity as a function of irradiation time. The Y-axis is reported as C/C_0, where C_0 and C are the initial and actual concentration of RhB at different reaction times. It can be clearly seen in Figs. 8 and 9a that under the identical test condition, uncoated PVP-capped ZnO showed much greater photocatalytic activity than silica-coated samples. For example, in the presence of uncoated PVP-capped ZnO, 98% of the dye was degraded at the irradiation time of 120 min, while it was only 57% and 45.4% in the presence of SCZN-18 and SCZN-24, respectively. Thus, the coating of silica on the surface of ZnO nanoparticles markedly suppressed the photodegradation of the RhB solution under the irradiation of simulated sunlight. As shown in Fig. 9b, the $\ln(C_0/C)$ plot shows a linear relationship with the irradiation time, which indicates that the photodegradation of the dye went through a pseudo-first-order kinetic reaction [25], i.e., $\ln(C_0/C)=kt$, where C_0 and C are the initial and actual concentration of RhB at time t, respectively, and k is the photodegradation rate constant. The photodegradation rate constants decreased from 0.016 min^{-1} for uncoated PVP-capped ZnO, to 0.010 min^{-1} for SCZNs-7, and finally reached 0.003 min^{-1} for SCZNs-18. Further increase in coating time did not change the photo-degradation rate constants (Fig. 9c). At the same time, the UV absorbance intensity at 350 nm decreased 15% during the first 7 h coating due to the loss of nanoparticles but remained

Fig. 8 Time-dependent absorption spectra of RhB solutions during simulated sunlight irradiation in the presence of silica–ZnO nanocomposites at different reaction times for silica coating; **a** 7, **b** 18, **c** 24, and **d** 48 h
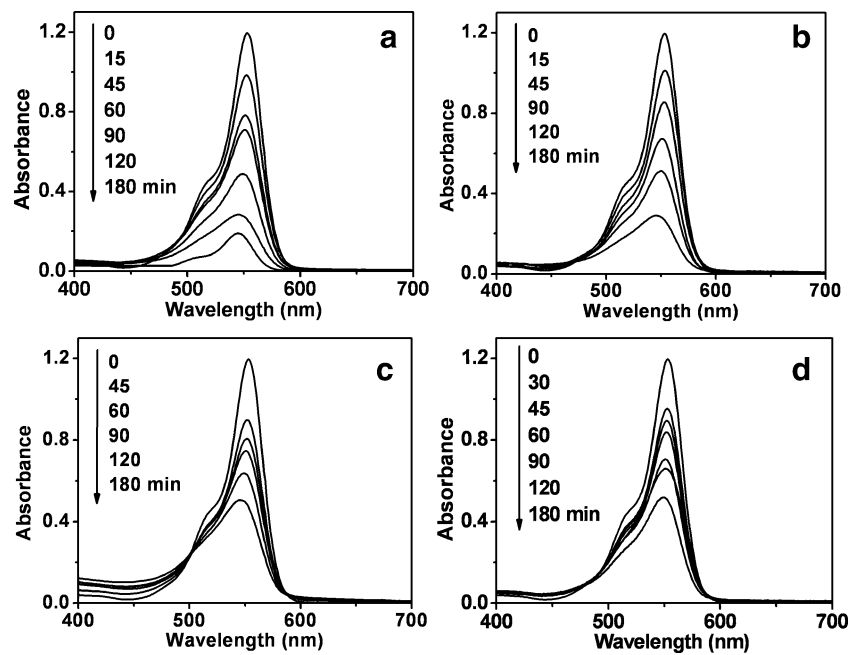

constant afterwards as shown in Fig. 9c. Taking into account these changes in the UV–vis absorbance and the photodegradation rate, it is concluded that the silica–ZnO nanocomposite can achieve optimum UV-blocking property after 20 h of aging time in the coating process.

Conclusions

The direct application of silica coating on ZnO particles is normally difficult due to the poor chemical stability of ZnO. In

this study, it was demonstrated that the use of PVP as a coupling agent enabled the formation of silica layers on ZnO nanoparticles. PVP was absorbed onto ZnO colloids during particle growth. During the silica coating process using the Stöber method, PVP acted as a dispersion stabilizer as well as a coupling agent for the formation of silica layers on ZnO. The mechanism of silica-layer development on PVP-capped ZnO nanoparticles was investigated using UV–vis and FT-IR spectroscopy. It is suggested that the formation of C–O⁻ groups in PVP molecules played an important role for the growth of ZnO nanoparticles. It is also suggested that the

Fig. 9 **a** Photocatalytic activity of silica–ZnO nanocomposites with different silica coating time as a function of irradiation time where C_0 and C are the initial and actual concentration of RhB at different reaction times, respectively, **b** the $\ln(C_0/C)$ vs irradiation time of RhB photodegradation over silica–ZnO nanocomposites with different silica coating time, and **c** UV–vis absorbance and degradation rate of silica-coated ZnO with different shell thickness
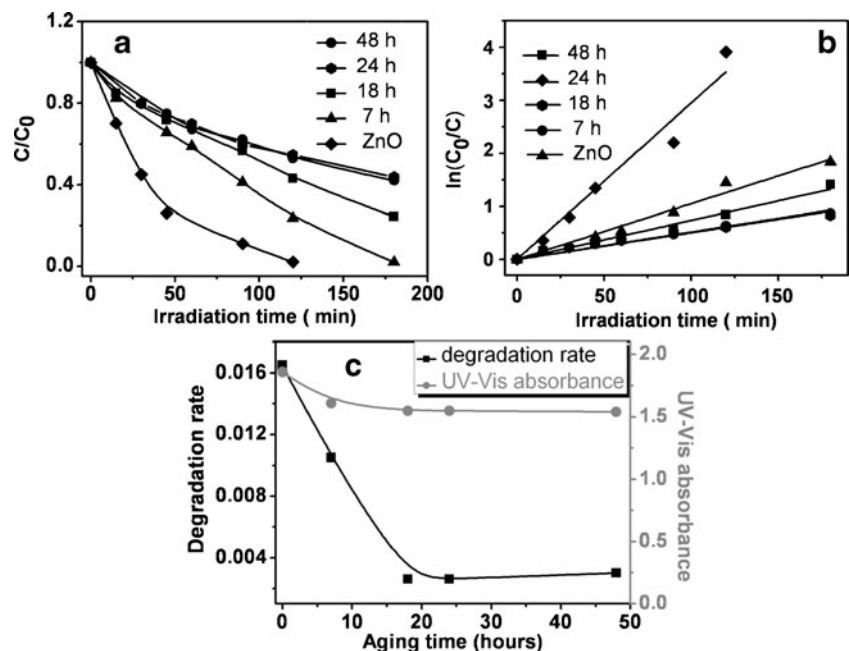
hydrogen bonding between the OH groups on hydrolyzed TEOS and C=O groups in PVP molecules was the key force for PVP to act as a coupling agent between ZnO and the silica layers. The thickness of the silica coatings on the surface of ZnO could be tuned by changing the aging time to hydrolyze TEOS. The silica-coated ZnO nanocomposites showed reduced photocatalytic activity with increased silica-layer thickness. This silica coating process allows control of the photocatalytic activity of ZnO nanoparticles and enables the applications of ZnO as a safe UV-blocking material.

References

1. Gerhard R, Werner H, Holger P, Heinrich S, Seidlitz HK, Hohn B (2000) Elevated UV-B radiation reduces genome stability in plants. Nature 406:98–101
2. Fernandez L, Garro N, Haskouri EJ, Perez-Cabero M, Alvarez-Rodriguez J, Latorre J, Guillem C, Beltran A, Beltran D, Amoros P (2008) Mesosynthesis of ZnO–SiO$_2$ porous nanocomposites with low-defect ZnO nanometric domains. Nanotechnology 19:10
3. Wang JF, Tsuzuki T, Sun L, Wang XG (2009) Reducing the photocatalytic activity of zinc oxide quantum dots by surface modification. J Am Ceram Soc 92:2083–2088
4. Hong RY, Pan TT, Qian JZ, Li HZ (2006) Synthesis and surface modification of ZnO nanoparticles. Chem Eng J 119:71–81
5. Siddiquey IA, Furusawa T, Sato M, Suzuki N (2008) Microwave-assisted silica coating and photocatalytic activities of ZnO nanoparticles. Mater Res Bull 43:3416–3424
6. Graf C, Vossen DLJ, Arnout I, Blaaderen AV (2003) A general method to coat colloidal particles with silica. Langmuir 19:6693–6700
7. Pattanaik M, Bhaumik SK (2000) Adsorption behaviour of polyvinyl pyrrolidone on oxide surfaces. Mater Lett 44:352–360
8. Smith JN, Meadows J, Williams PA (1996) Adsorption of polyvinylpyrrolidone onto polystyrene latices and the effect on colloid stability. Langmuir 12:3773–3778
9. Esumi K, Matsui H (1993) Adsorption of non-ionic and cationic polymers on silica from their mixed aqueous solutions. Colloids Surf, A 80:273–278
10. Otsuka H, Esumi K (1995) Interaction between poly(N-vinyl-2-pyrrolidone) and anionic hydrocarbon/fluorocarbon surfactant on hydrophobic graphite. J Colloid Interface Sci 170:113–119
11. Luo Y, Dai C, Chiu W (2008) Synthesis of P(AA-SA)/ZnO composite latex particles via inverse miniemulsion polymerization and its application in pH regulation and UV shielding. J Polym Sci A Poly Chem 46:8081–8090
12. Becheri A, Dürr M, Nostro PL, Baglioni P (2008) Synthesis and characterization of zinc oxide nanoparticles. J Nanopart Res 10:679
13. Wang RH, Xin JH, Tao XM (2005) UV-blocking property of dumbbell-shaped ZnO crystallites on cotton fabrics. Inorg Chem 44:3926
14. Sun L, Rippon JA, Cookson PG, Wang XG, King K, Koulaeva O, Beltrame R (2008) Nano zinc oxide for UV protection of textiles. Int J Tech Trans Commerc 7:224–235
15. Dunford R, Salinaro A, Cai L, Serpone N, Horikoshi S, Hidaka H, Knowland J (1997) Chemical oxidation and DNA damage catalysed by inorganic sunscreen ingredients. FEBS Lett 418:87–90
16. Stober W, Fink A, Bohn E (1968) Controlled growth of monodisperse silica spheres in the micron size range. J Colloid Interface Sci 26:62–69
17. Noda I, Ozaki Y (2004) Two-dimensional correlation spectroscopy: applications in vibrational and optical spectroscopy. Wiley, Chichester
18. Yamada A, Miyazaki H, Chiba Y, Konagai M (2005) High-efficiency Cu(InGa)Se$_2$ solar cells with a zinc-based buffer layer. Thin Solid Films 480–481:503–508
19. Doussineau T, Smaïhi M, Mohr GJ (2009) Two-dye core/shell zeolite nanoparticles: a new tool for ratiometric pH measurements. Adv Funct Mater 19:117–122
20. Sui X, Shao C, Liu Y, Xu C (2006) Structural and photoluminescent properties of ZnO hexagonal nanoprisms synthesized by microemulsion with polyvinyl pyrrolidone served as surfactant and passivant. Chem Phys Lett 424:340–344
21. Maensiri S, Laokul P, Promarak V (2006) Synthesis and optical properties of nanocrystalline ZnO powders by a simple method using zinc acetate dihydrate and poly(vinyl pyrrolidone). J Cryst Growth 289:102–106
22. Zhang Q, Ge J, Yin Y (2008) Permeable silica shell through surface-protected etching. Nano Lett 8:2867–2871
23. Hong P, Huang HT (2000) Effect of co-solvent complex on preferential adsorption phenomenon in polyvinyl alcohol ternary solutions. Polymer 41:6195–6204
24. Kajimoto N, Manaka T, Iwamoto M (2006) Electrostatic energies stored in dipolar films and analysis of decaying process of a large surface potential of Alq$_3$ films. Chem Phys Lett 430:340–344
25. Wan Q, Wang TH, Zhao JC (2005) Enhanced photocatalytic activity of ZnO nanotetrapods. Appl Phys Lett 87:083105